

# Random Matrix Theory and QCD at nonzero chemical Potential

J.J.M. Verbaarschot<sup>a</sup>

<sup>a</sup>Department of Physics and Astronomy,  
University at Stony Brook,  
Stony Brook, NY 11794, USA

In this lecture we give a brief review of chiral Random Matrix Theory (chRMT) and its applications to QCD at nonzero chemical potential. We present both analytical arguments involving chiral perturbation theory and numerical evidence from lattice QCD simulations showing that correlations of the smallest Dirac eigenvalues are described by chRMT. We discuss the range of validity of chRMT and emphasize the importance of universality. For chRMT's at  $\mu \neq 0$  we identify universal properties of the Dirac eigenvalues and study the effect of quenching on the distribution of Yang-Lee zeros.

## 1. INTRODUCTION

There are strong indications from hadronic phenomenology that chiral symmetry is broken spontaneously at low temperatures. However, mainly through lattice QCD simulations, it has become generally accepted that chiral symmetry is restored above a critical temperature of about  $140 \text{ MeV}$  (see reviews by DeTar [1], Ukawa [2], Smilga [3] and Karsch [4] for recent results on this topic). The situation at nonzero chemical potential is much less clear. Because of the phase of the fermion determinant it is not possible to perform Monte-Carlo simulations, and it seems that one has to give up calculations based on first principles. It is certainly not possible to make progress by a gradual improvement of existing techniques. Instead, radically different approaches have to be developed.

The main source of the problem is the loss of Hermiticity at nonzero chemical potential. In this lecture we study this problem by means of a much simpler chiral Random Matrix Theory (chRMT) with the global symmetries of the Dirac operator [5–8]. This model has the remarkable property that, in spite of the fact that it can be solved analytically, it cannot be solved numerically. In the broken phase, numerical convergence is only obtained for an exponentially large ensemble [9]. If one is not able to develop an algorithm for this simple model, progress in QCD will be elusive.

Originally, chRMT was introduced to describe the correlations of QCD Dirac eigenvalues. Our interest in the Dirac spectrum is based on the relation between the chiral condensate,  $\Sigma$ , and the spectral density per unit of space time volume,  $V$ , given by  $\Sigma = \lim \pi \rho(0)/V$  [10]. Note that the thermodynamic limit has to be taken before the chiral limit. The spectral density is defined by  $\rho(\lambda) = \sum_k \delta(\lambda - \lambda_k)$ , where the  $\lambda_k$  are the eigenvalues of the Dirac operator. Because of this relation the eigenvalues near zero are spaced as  $1/\rho(0) = \pi/\Sigma V$ . In order to study the approach to the thermodynamic limit it

is natural to introduce the microscopic limit in which  $u = \lambda V \Sigma$  is kept fixed for  $V \rightarrow \infty$ , and the microscopic spectral density [5]

$$\rho_S(u) = \lim_{V \rightarrow \infty} \frac{1}{V \Sigma} \langle \rho(\frac{u}{V \Sigma}) \rangle. \quad (1)$$

Our claim is that the microscopic spectral density of the QCD Dirac operator is given by chRMT. This has been confirmed both by analytical arguments using partially quenched chiral perturbation theory [11], and lattice QCD [12–16] and instanton liquid [17,18] simulations. In addition to this, correlations in the bulk of the spectrum are given by chRMT [19–21,15] as well. Random matrix theory can describe only those observables which are universal, i.e., which are stable against large deformations of the random matrix ensemble. By now it has been well established that both the microscopic spectral density and the spectral correlations are strongly universal [22–29], [30]. Before discussing the random matrix model at nonzero chemical potential, we wish to establish the domain of applicability of chRMT at  $\mu = 0$ . Starting from partially quenched Chiral Perturbation Theory [31] we will argue that, below a scale of  $\Lambda_{QCD}/\sqrt{V}$ , eigenvalue correlations are given by chRMT. This scale is the equivalent of the Thouless energy in mesoscopic physics (see [32–34] for recent reviews). The existence of such a scale has been confirmed by lattice QCD [14,15] and instanton liquid [18] simulations. The interpretation is that the classical motion of the quarks in the background gauge fields is chaotic.

Before proceeding to the main body of this talk, let me stress that there are two different types of applications of RMT. First, as the simplest model of a universality class, and second, as a schematic model for a complex system. Typical examples in the first class are related to eigenvalue correlations [32]. Perhaps, the most famous example in the second class is the Anderson model for localization [35]. In this lecture we will discuss a schematic RMT model for the chiral phase transition at nonzero chemical potential.

## 2. CHIRAL RANDOM MATRIX THEORY

In this section we will introduce an instanton liquid [36,37] inspired chiral RMT for the QCD partition function. With only its global symmetries as input but otherwise Gaussian distributed matrix elements the chRMT for  $N_f$  flavors and topological charge  $\nu$  is defined by [5,38]

$$Z_{N_f, \nu}^\beta(m_1, \dots, m_{N_f}) = \int DW \prod_{f=1}^{N_f} \det(\mathcal{D} + m_f) e^{-\frac{N \Sigma^2 \beta}{4} \text{Tr} W^\dagger W}, \quad (2)$$

where

$$\mathcal{D} = \begin{pmatrix} 0 & iW \\ iW^\dagger & 0 \end{pmatrix}, \quad (3)$$

and  $W$  is a  $n \times m$  matrix with  $\nu = |n - m|$  and  $N = n + m$ . We interpret  $N$  as the (dimensionless) volume of space time. The matrix elements of  $W$  are either real ( $\beta = 1$ , chiral Gaussian Orthogonal Ensemble (chGOE)), complex ( $\beta = 2$ , chiral Gaussian Unitary Ensemble (chGUE)), or quaternion real ( $\beta = 4$ , chiral Gaussian Symplectic Ensemble (chGSE)). As is the case in QCD, we assume that  $\nu$  does not exceed  $\sqrt{N}$ , so that, to a

good approximation,  $n = N/2$ . The Dyson index  $\beta$  of a physical system is determined by its anti-unitary symmetries. If the square of the anti-unitary symmetry operator is equal to the identity, we have  $\beta = 1$ . If its square is equal to minus the identity, we have  $\beta = 4$ . If there no anti-unitary symmetries, the value of  $\beta = 2$ .

In this model chiral symmetry is broken spontaneously with chiral condensate given by  $\Sigma = \lim_{N \rightarrow \infty} \pi \rho(0)/N$ . For complex matrix elements ( $\beta = 2$ ), which is appropriate for QCD with three or more colors and fundamental fermions, the symmetry breaking pattern is  $SU(N_f) \times SU(N_f)/SU(N_f)$  [5,39].

The average spectral density that follows from (2) has the familiar semi-circular shape. The microscopic spectral density can be derived from the limit (1) of the exact spectral density for finite  $N$ . For  $N_c = 3$ ,  $N_f$  flavors and topological charge  $\nu$  it is given by [40,38]

$$\rho_S(z) = \frac{z}{2} \left( J_a^2(z) - J_{a+1}(z)J_{a-1}(z) \right), \quad (4)$$

where  $a = N_f + |\nu|$ . The spectral correlations in the bulk of the spectrum are given by the invariant random matrix ensemble with the same value of  $\beta$  [41,42].

The description of an observable in terms of chRMT is based on universality, i.e. on the stability against deformations of the random matrix ensemble. At this moment I only mention the work of Akemann, Damgaard, Magnea and Nishigaki [22] who showed that the same microscopic spectral density (4) is obtained for an invariant probability distribution defined by an arbitrary polynomial potential. The essence of their proof is a remarkable generalization of the identity for the Laguerre polynomials,  $\lim_{n \rightarrow \infty} L_n(x/n) = J_0(2\sqrt{x})$ , to orthogonal polynomials determined by the probability distribution.

### 3. DOMAIN OF VALIDITY

The domain of validity of chRMT is best discussed within the context of partially quenched chiral perturbation theory [31,11]. This is an effective field theory for the low-energy limit of a QCD like theory which, in addition to the usual  $N_f$  sea quarks, contains  $k$  valence quarks with mass  $m_v$  and their super-symmetric partners with the same mass. In this framework it is possible to calculate the valence quark mass dependence of the chiral condensate which is defined as

$$\Sigma_v(m_v) = \frac{1}{N} \int d\lambda \langle \rho(\lambda) \rangle \frac{2m_v}{\lambda^2 + m_v^2}. \quad (5)$$

The spectral density follows from the discontinuity of  $\Sigma_v(m_v)$ ,

$$\frac{2\pi}{N} \langle \rho(\lambda) \rangle = \text{Disc}|_{m_v=i\lambda} \Sigma(m_v) \equiv \lim_{\epsilon \rightarrow 0} \Sigma(i\lambda + \epsilon) - \Sigma(i\lambda - \epsilon) = \frac{2\pi}{N} \sum_k \langle \delta(\lambda + \lambda_k) \rangle, \quad (6)$$

where the average  $\langle \cdots \rangle$  is with respect to the distribution of the eigenvalues. Similarly, the two-point spectral correlation function, given by

$$\langle \rho(\lambda) \rho(\lambda') \rangle = \frac{1}{4\pi^2} \text{Disc}|_{m_v=i\lambda, m_{v'}=i\lambda'} \sum_{k,l} \left\langle \frac{1}{i\lambda_k + m_v} \frac{1}{i\lambda_l + m_{v'}} \right\rangle, \quad (7)$$

is related to the scalar susceptibility. Both the valence quark mass dependence of the chiral condensate and the scalar susceptibility can be calculated from the pqChPT partition

function. In both cases we can identify an important scale where the mass of the Goldstone modes containing a valence quark is equal to the inverse length of the box [43,44]. Using the relation  $M = (m + m')\Sigma/F^2$ , where  $F$  is the pion decay constant, we find from  $ML = 1$  that, in terms of the valence quark mass  $m_v$ , this scale is given by [18,45]

$$E_c = \frac{F^2}{\Sigma L^2}. \quad (8)$$

For  $m_v \ll E_c$  we have shown that the valence quark mass dependence and the scalar susceptibility can be obtained from the zero-momentum component of the pqChPT partition function and are given by the result for chRMT. The conclusion is that, if pqChPT describes correctly the low energy limit of QCD, we have shown that the correlations of the Dirac eigenvalues close to zero are given by chRMT.

Such a picture is well-known from mesoscopic physics. In this context  $E_c$  is defined as the inverse tunneling time of an electron through the sample which is given by  $E_c = \hbar D/L^2$ , where  $D$  is the diffusion constant. Another scale that enters in these systems is the elastic scattering time  $\tau_e$ . Based on these scales one can distinguish three different regimes for the energy difference,  $\delta E$ , that enters in the two-point correlation function [46]: i) the ergodic regime for  $\delta E \ll E_c$ , ii) the diffusive domain for  $E_c \ll \delta E \ll \hbar/\tau_e$  and iii) the ballistic regime for  $\delta E \gg \hbar/\tau_e$ . On time scales corresponding to the ergodic regime an initially localized wave packet covers all of phase space. In this domain the eigenvalue correlations are given by RMT. On time scales corresponding to the diffusive domain an initially localized wave packet explores only part of the phase space resulting in eigenstates with wavefunctions that are localized in different regions. The corresponding eigenvalues show weaker correlations which are no longer given by RMT. For earlier applications of localization theory to the chiral phase transition we refer to [47].

Based on these ideas we can interpret the Dirac spectrum as the energy levels of a system in four Euclidean dimensions and one artificial time dimension. According to the Bohigas conjecture [48] the eigenvalue correlations are given by RMT if and only if the corresponding classical motion is chaotic. We thus conclude that the classical time evolution of quarks in the Yang-Mills gauge fields is chaotic.

These ideas have been tested by means of lattice QCD [14,15] and instanton liquid [18] simulations. It has been found that the eigenvalue correlations are given by chRMT up to the predicted scale of  $E_c = F^2/\Sigma L^2$ .

#### 4. LATTICE QCD RESULTS

In this section we consider correlations of lattice QCD Dirac eigenvalues. For a Dirac operator with a  $U_A(1)$  symmetry the eigenvalues occur in pairs  $\pm\lambda_k$ . Therefore we have to distinguish two different regions: the region near zero virtuality and the bulk of the spectrum. The  $U_A(1)$  symmetry is absent for the Hermitean Wilson Dirac operator.

The class of random matrix ensembles is determined by anti-unitary symmetries. In the case of an  $SU(2)$  color group, the anti-unitary symmetries of the Kogut-Susskind (KS) and the Wilson Dirac operator are given by [49,19],

$$[D^{KS}, \tau_2 K] = 0, \quad \text{and} \quad [\gamma_5 D^W, \gamma_5 C K \tau_2] = 0. \quad (9)$$

Because  $(\tau_2 K)^2 = -1$  and  $(\gamma_5 C K \tau_2)^2 = 1$ , we find a Dyson index  $\beta = 1$  for Wilson fermions and  $\beta = 4$  for KS fermions. The KS Dirac operator for two colors is thus described by the chGSE. In the absence of a  $U_A(1)$  symmetry, the Wilson Dirac operator for two colors is described by the GOE [19]. For three or more colors there are no anti-unitary symmetries and the relevant ensembles are the chGUE and GUE for KS and Wilson fermions, respectively.

In order to separate the correlations from the average spectral density, the eigenvalues are rescaled according to the local average level spacing. Under the assumption of spectral ergodicity, eigenvalue correlations in the bulk of the spectrum can be calculated by spectral averaging instead of ensemble averaging. For subtle differences between the two we refer to [15]. Eigenvalues calculated by Kalkreuter [50] for the  $N_c = 2$  KS and Wilson Dirac operators for lattices as large as  $12^4$  have been analyzed by means of spectral averaging [19,20]. For different values of  $\beta$ , ranging from strong coupling to weak coupling, it was found that correlations are in complete agreement with chRMT for distances as large as 100 level spacings. Recently, correlations in the bulk of the spectrum were also investigated for  $N_c = 3$  [21,51]. Agreement with chRMT was even found for values of  $\beta$  well above the deconfinement transition. For a discussion of global Wilson spectra we refer to [52,53].

Spectral ergodicity cannot be exploited in the study of the microscopic spectral density. In order to gather sufficient statistics one has to generate a large number of independent QCD Dirac spectra. The analysis of these spectra convincingly shows that the smallest

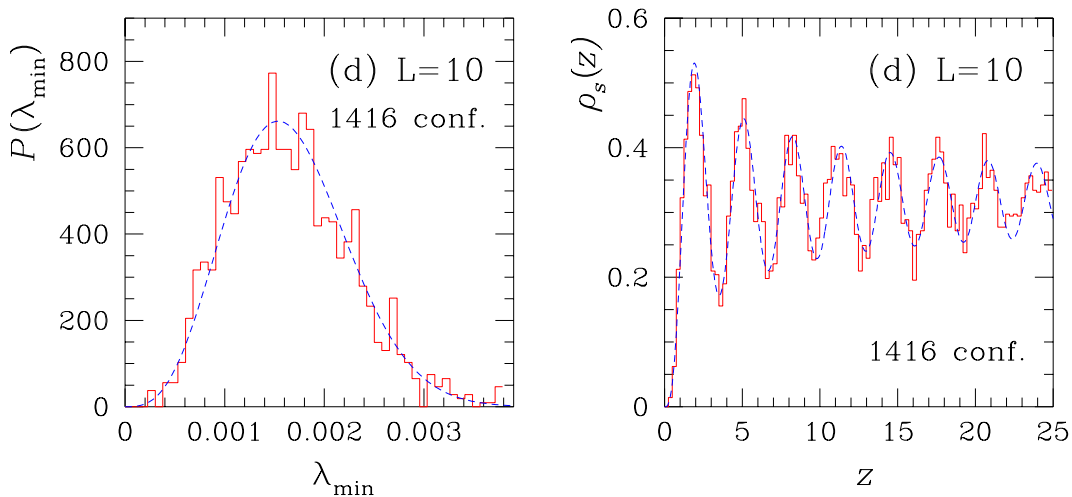


Figure 1. The distribution of the smallest eigenvalue (left) and the microscopic spectral density (right) of the Kogut-Susskind Dirac operator for two colors and  $\beta = 2.0$ .

eigenvalues are correlated according to chRMT [12–14,16,15]. Results for 1416 configurations [12] on  $10^4$  lattice for  $\beta = 2$  are shown in Fig. (1). For more detailed results, including results for the two-point correlation function, we refer to the original work. In Fig. 4 we show the distribution of the smallest eigenvalue (left) and the microscopic spectral density (right). The lattice results are given by the full line. The dashed curves represent the random matrix results. We emphasize that the theoretical curves have been obtained without any fitting of parameters. The input parameter, the chiral condensate, is derived from the same lattice calculations. Recently, the same analysis [12] was per-

formed for  $\beta = 2.2$  and for  $\beta = 2.5$  on a  $16^4$  lattice. In both cases agreement with the random matrix predictions was found [12].

It is an interesting question of how spectral correlations of KS fermions evolve in the approach to the continuum limit. Certainly, the Kramers degeneracy of the eigenvalues remains. However, since Kogut-Susskind fermions represent 4 degenerate flavors in the continuum limit, the Dirac eigenvalues should obtain an additional two-fold degeneracy. We are looking forward to more work in this direction.

## 5. APPLICATIONS OF chRMT AT $\mu \neq 0$

In the continuum formulation of QCD the chemical potential enters in the QCD partition function by the addition of the term  $\mu\gamma_0$  to the anti-Hermitian Dirac operator, i.e.  $\mathcal{D} \rightarrow \mathcal{D} + \mu\gamma_0$ . In a suitable chiral basis, in which the matrix elements of  $\langle \phi_R^k | \gamma_0 | \phi_L^k \rangle = \delta_{kl}$ , the corresponding modification in the random matrix partition function (2) is to replace the Dirac matrix  $\mathcal{D}$  by [8]

$$\mathcal{D}(\mu) = \begin{pmatrix} 0 & iW + \mu \\ iW^\dagger + \mu & 0 \end{pmatrix}. \quad (10)$$

As is the case in QCD, a nonzero chemical potential violates the anti-Hermiticity of the Dirac operator and its eigenvalues are scattered in the complex plane. For three or more colors this results in a complex fermion determinant. The presence of this phase makes it virtually impossible to perform Monte-Carlo simulations for the full theory. The easy way out would be to ignore the fermion determinant altogether. However, it was shown that the quenched approximation fails dramatically [55–57]. The critical chemical potential is determined by the pion mass instead of the nucleon mass. After some earlier work by [58,59] this puzzle was resolved convincingly by Stephanov [8] within the context of chRMT at  $\mu \neq 0$ . He could show analytically that the quenched approximation is not the  $N_f \rightarrow 0$  limit of the full theory but rather the  $N_f \rightarrow 0$  limit of a theory in which the fermion determinant is replaced by its absolute value. This theory can be interpreted as a theory that contains an equal number of quarks and conjugate quarks. It was shown that in this theory chiral symmetry is broken spontaneously by the formation of a quark conjugate anti-quark condensate. The critical chemical potential is then determined by the mass of the corresponding Goldstone bosons with a net baryon number.

Because the term  $\mu\gamma_0$  does not change the anti-unitary symmetries of the Dirac operator the classification for  $\mu = 0$  is also valid at  $\mu \neq 0$ . For example, the Kogut-Susskind Dirac operators for  $N_c \geq 3$  and  $N_c = 2$  corresponds to the classes  $\beta = 2$  and  $\beta = 4$ , respectively, whereas the continuum Dirac operator for  $N_c = 2$  corresponds to  $\beta = 1$ .

The fermion determinant is real both for  $\beta = 1$  and  $\beta = 4$ . This is obvious for  $\beta = 1$ . For  $\beta = 4$  the reality follows from the identity  $q^* = \sigma_2 q \sigma_2$  for a quaternion real element  $q$ , and the invariance of a determinant under transposition. We thus conclude that Monte-carlo simulations can be performed for  $\beta = 1$  and  $\beta = 4$ . For these values of  $\beta$  the partition function can also be interpreted in terms of quarks and conjugate quarks and chiral symmetry will be restored for arbitrarily, small nonzero  $\mu$ , whereas a condensate of a quark and a conjugate anti-quark develops. Indeed, this phenomenon has been observed in the strong coupling limit of lattice QCD with two colors [60].

Alternatively, one may write  $\det \mathcal{D} + m = \det \gamma_0(\mathcal{D} + m)$  with the fermion matrix [61]

$$\gamma_0(\mathcal{D}(\mu) + m) = \begin{pmatrix} iW + \mu & m \\ m & iW^\dagger + \mu \end{pmatrix}. \quad (11)$$

Let us study this model for  $m = 0$ . In terms of the eigenvalues,  $\lambda_k$ , of  $W$  the baryon number density is simply given by

$$n_q = \frac{1}{N} \sum_k \left[ \frac{1}{\lambda_k + \mu} + \frac{1}{\lambda_k^* + \mu} \right]. \quad (12)$$

A natural electrostatic interpretation of this result is that  $n_q$  is the electric field at location  $\mu$  due to charges located at the positions of the eigenvalues. As was shown by Ginibre [62], the eigenvalues of  $W$  are distributed homogeneously in a disk in the complex plane. For small  $\mu$  we thus have that  $n_q \sim \mu$  in the quenched approximation.

For unquenched QCD we expect that  $n_q = 0$  for  $\mu < \mu_c \neq 0$ . By the electrostatic analog this is only possible if there are no eigenvalues in the domain  $\mu < \mu_c$ . The effect of the fermion determinant is to average the spectral density of  $W$  to zero in this region. In the random matrix model the phase of the fermion determinant does not result in a zero baryon density below  $\mu_c$ . Instead,  $n_q$  becomes negative. The reason is that chRMT is a schematic model for the chiral phase transition in which the low temperature behavior has not been implemented correctly. The claim is that taking into account all Matsubara frequencies will restore this deficiency [54].

This RMT partition function at  $\mu \neq 0$  has inspired a great deal of interest. For recent literature on this topic we refer to [63,64,54,9].

### 5.1. Yang-Lee Zeros of the Partition Function

In this section we discuss the distribution of Yang-Lee zeros [65] in the complex  $\mu$  plane. In particular, we compare the zeros of the unquenched partition function for  $N_f = 2$  and of the partition function with one flavor and one conjugate flavor (which we will denote by  $N_f = 1+1^*$ ). A recent controversial question raised in [66] is whether the phase quenched partition function with  $N_f = 1+1^*$  can teach us something about the full theory. Zeros of polynomials have been studied elaborately in the mathematics literature. At this moment we only mention a limit theorem for the distribution of zeros of polynomials with random coefficients which states that it converges to the complex unit circle (see for example [67]).

Since the chRMT partition function is a polynomial in  $\mu$  it can be factorized as

$$Z = \prod_k (\mu - \mu_k), \quad (13)$$

where the  $\mu_k$  are the complex zeros of the partition function. The baryon number density is thus given by [68,69]

$$n_q = \frac{1}{N} \sum_k \frac{1}{\mu - \mu_k}, \quad (14)$$

and can be interpreted as the electric field at the position  $\mu$  from charges located at  $\mu_k$  in two dimensional complex  $\mu$ -plane.

In QCD at  $T = 0$ , we expect that  $n_q = 0$  for  $\mu < \mu_c$  which is only possible if, in the thermodynamic limit, the number of zeros with absolute value less than  $\mu_c$  become negligible with respect to the total number of zeros. At  $\mu_c$  we expect a first order phase transition with a discontinuity in the baryon number density. In terms of the zeros, this implies that they should coalesce into to a cut for  $N \rightarrow \infty$ . In order to have  $n_q = 0$  for  $|\mu| < \mu_c$ , this cut has necessarily to be a circle of radius  $\mu_c$ . Since the low-temperature limit has not been implemented correctly in our schematic model we will find a different curve for the location of the zeros.

In terms of the  $\sigma$ -representation the random matrix partition function for  $N_f$  flavors can be rewritten

$$Z^{N_f}(m = 0, \mu) = \int \mathcal{D}\sigma \exp[-n\Sigma^2 \text{Tr}\sigma\sigma^\dagger] \det^n(\sigma\sigma^\dagger - \mu^2) \quad (15)$$

where  $\sigma$  is an arbitrary complex  $N_f \times N_f$  matrix. Since the value of the chiral condensate is given by the expectation value of  $\sigma$ , the logarithm of the integrand can be interpreted as a Landau-Ginzburg functional for the order parameter. From a saddle-point analysis it follows that this partition function describes a first order phase transition [8]. Since the equality of the real part of the free energies on opposite sides of the phase boundary imposes one condition on the value of  $\mu$  in the complex plane, the phase boundary is given by a curve in the complex plane [70]. In the thermodynamic limit the zeros that are located on this curve should join into a cut. The result for this curve given by [8,9]

$$\text{Re}[\mu^2 + \log(\mu^2)] = -1 \quad (16)$$

is represented by the solid curve within the complex unit circle in Fig. (2). It does not depend on the number of flavors for  $n \rightarrow \infty$ .

The  $\sigma$ -model representation of the partition function for one flavor and one conjugate flavor is given by

$$Z^{1+1^*}(m = 0, \mu) = \int \mathcal{D}\sigma \exp[-n\Sigma^2 \text{Tr}\sigma\sigma^\dagger] \det^n(\sigma k \sigma^\dagger k - \mu^2), \quad (17)$$

where  $\sigma$  is an arbitrary complex  $2 \times 2$  matrix and  $k \equiv \sigma_3$ . This partition function is an exact rewriting of the partition function (2) for  $N_f = 2$  with (10) but with the determinant replaced by its absolute value. For even  $n$  this partition function is invariant under  $\sigma \rightarrow \sigma\sigma_1$  and  $\mu \rightarrow i\mu$ . As a consequence it can be factorized as a polynomial in  $\mu^4$ .

The numerical results for the zeros of the partition function for  $N_f = 2$  (left) and  $N_f = 1 + 1^*$  (right) are depicted by the full circles in Fig. (2). In both cases the total number of zeros is equal to 320. They were obtained with the help of a multi-precision package [71]. Typically, we performed our computations with about 500 significant digits. In both cases the complex zeros duplicate the result for the thermodynamic limit. For two flavors, the zeros join into two curves which are separated by  $\sim 1/\sqrt{n}$  for large  $n$  and approach the analytical result (16). Remarkably, half of the zeros coincide almost exactly with (16). The picture is quite different for  $N_f = 1 + 1^*$ . In this case we observe doubly degenerate zeros that approach (16), that approach (16) rotated by 90 degrees, and isolated zeros that are located along the diagonals. The fraction of zeros in each of these three sets remains finite in the thermodynamic limit. In this figure, the total number in each set is given by, 120, 120 and 80, respectively. Of course, this pattern



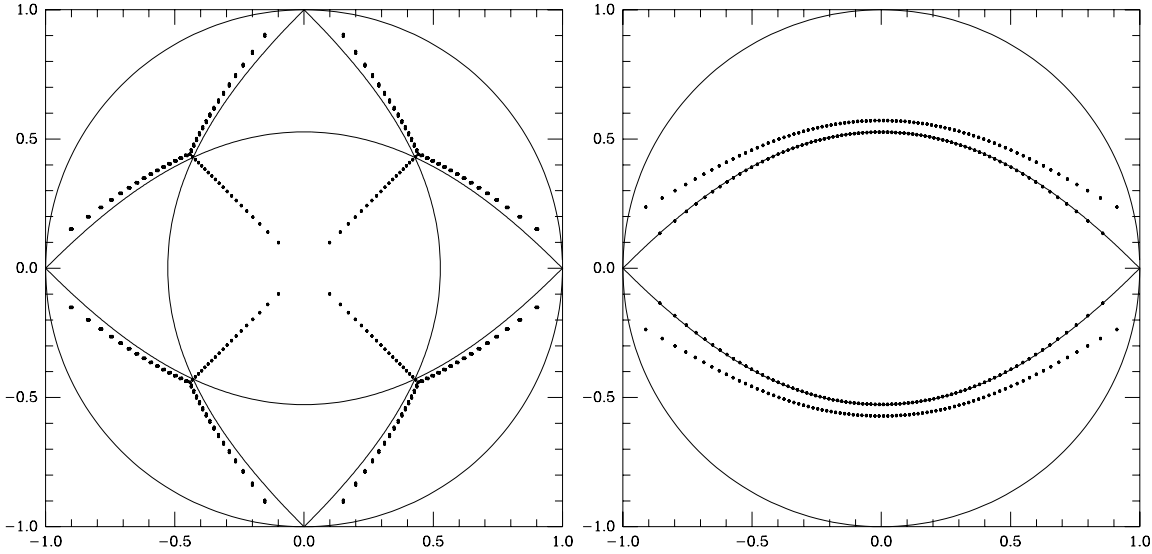


Figure 2. Yang-Lee zeros of the RMT partition function with  $N_f = 1 + 1^*$  (left) and  $N_f = 2$  (right).

reflects that for  $N_f = 1 + 1^*$  the polynomial is a polynomials in  $\mu^4$ . The vertical axis represents the real  $\mu$  axis. For  $N_f = 2$  we observe a second order phase transition at  $\mu_c \approx 0.52$ . This result can also be obtained by an extrapolation of the distribution of the zeros of the  $N_f = 1 + 1^*$  partition function. We conclude that this partition function contains information of the full theory. For  $N_f = 1 + 1^*$  the density of the zeros decreases linearly with the distance to the imaginary axis which is typical for a second order phase transition.

## 5.2. Phase Diagram

In the random matrix model one can include a schematic temperature dependence by the substitution  $\mu \rightarrow \mu + iT$ . In this case the  $\sigma$ - model representation of the partition function is given by [72]

$$Z(m, \mu, T) = \int d\sigma e^{-N\mathcal{L}(\sigma)} \quad (18)$$

where  $\mathcal{L}(\sigma)$  is given by

$$\mathcal{L}(\sigma) = \text{Tr}[\sigma\sigma^\dagger - \frac{1}{2} \ln\{[(\sigma + m)(\sigma^\dagger + m) - (\mu + iT)^2] \cdot [(\sigma + m)(\sigma^\dagger + m) - (\mu - iT)^2]\}]$$

and  $\sigma$  is an arbitrary complex  $N_f \times N_f$  matrix. This model was studied for  $\mu = 0$  in [6,7,73]. It was found that it describes a second order phase transition at a nonzero temperature. Multicritical behavior was studied in [74–77]. At zero temperature, a first order phase transition [8] was found at  $\mu \neq 0$ .

Since, the value order parameter is given by the expectation value  $\sigma$ , this partition function can be interpreted as a Landau-Ginzburg functional. A similar functional can be derived from a Nambu model [78]. It possesses a tricritical point at  $m = 0$ ,  $\mu = \mu_3$  and  $T = T_3$ . The critical exponents at this point are given by the universal mean field critical exponents. We emphasize that the upper critical dimension at the tricritical point is equal to 3 so that up to logarithmic corrections, the mean field critical exponents are exact.

For a detailed discussion of the phase structure of this partition function and the physics of the tricritical point [79] we refer to the talk by M. Stephanov [80] in this volume. For other studies of the RMT partition function at nonzero  $\mu$  and  $T$  we refer to [54].

### 5.3. Random Matrix Triality at Nonzero Chemical Potential

In this section, we provide evidence that the RMT Dirac operator at  $\mu \neq 0$  shows universal behavior as well. In particular, we will consider the chRMT partition function for all three values of  $\beta$  and show that the anti-unitary symmetries of the Dirac operator result in characteristic eigenvalue correlations.

Numerical simulations have been performed for all three classes. A cut along the imaginary axis below a cloud of eigenvalues was found in instanton liquid simulations [81] for  $N_c = 2$  at  $\mu \neq 0$  which corresponds to  $\beta = 1$ . In lattice QCD simulations with staggered fermions for  $N_c = 2$  [82] a depletion of eigenvalues along the imaginary axis was observed, whereas for  $N_c = 3$  the eigenvalue distribution did not show any pronounced features [55].

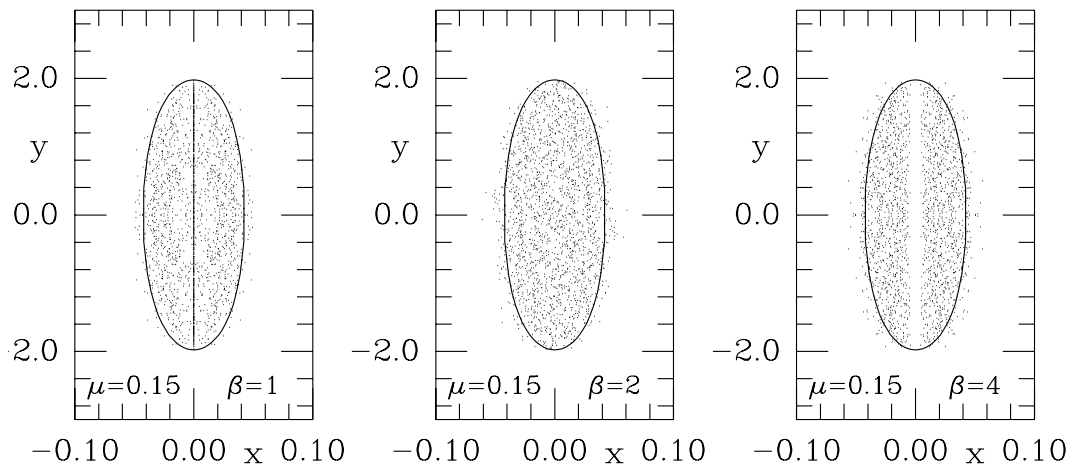


Figure 3. Scatter plot of the real ( $x$ ), and the imaginary parts ( $y$ ) of the eigenvalues of the random matrix Dirac operator.

In the quenched approximation, the spectral properties of the random matrix Dirac operator (10) can easily be studied numerically by diagonalizing a set of matrices with probability distribution (2). In Fig. (3) we show results [83] for the eigenvalues of a few  $100 \times 100$  matrices for  $\mu = 0.15$  (dots). The solid curve represents the analytical result for the boundary of the domain of eigenvalues derived in [8] for  $\beta = 2$ . However, the method that was used can be extended [83] to  $\beta = 1$  and  $\beta = 4$  and with the proper scale factors we find exactly the same solution.

For  $\beta = 1$  and  $\beta = 4$  we observe exactly the same structure as in the previously mentioned (quenched) simulations. We find an accumulation of eigenvalues on the imaginary axis for  $\beta = 1$  and a depletion of eigenvalues along this axis for  $\beta = 4$ . This depletion can be understood as follows. For  $\mu = 0$  all eigenvalues are doubly degenerate. This degeneracy is broken at  $\mu \neq 0$  which produces the observed repulsion between the eigenvalues.

The number of purely imaginary eigenvalues for  $\beta = 1$  scales as  $\sqrt{N}$  and is thus not visible in a leading order saddle point analysis. Such a  $\sqrt{N}$  scaling is typical for the regime

of weak non-hermiticity first identified by Fyodorov *et al.* [84]. Using the supersymmetric method of random matrix theory the  $\sqrt{N}$  dependence was obtained analytically by Efetov [85]. Obviously, more work has to be done in order to arrive at a complete characterization of universal features [86] in the spectrum of nonhermitean matrices.

## 6. CONCLUSIONS

There is strong evidence from lattice QCD simulations and partially quenched chiral perturbation theory that eigenvalue correlations below a scale of  $F^2/\Sigma\sqrt{V}$  are given by chRMT. We emphasize that this is an exact result. On the other hand, qualitative results have been obtained for a schematic chRMT model for the chiral phase transition at nonzero chemical potential and temperature. We have discussed the mechanism of quenching and the distribution of the Yang-Lee zeros and found that the phase quenched partition function contains information of the critical chemical potential of the full theory.

## Acknowledgements

This work was partially supported by the US DOE grant DE-FG-88ER40388. Frithjof Karsch and Maria-Paola Lombardo are thanked for organizing this workshop. We benefited from discussions with P. Damgaard, T. Guhr, A. Jackson, A. Schäfer, M. Stephanov, T. Wettig and H. Weidenmüller. J. Osborn is thanked for a critical reading of the manuscript. Finally, I thank my collaborators on whose work this review is based.

## REFERENCES

1. C. DeTar, *Quark-gluon plasma in numerical simulations of QCD*, in *Quark gluon plasma 2*, R. Hwa ed., World Scientific 1995.
2. A. Ukawa, Nucl. Phys. Proc. Suppl. **53** (1997) 106. Lattice 1996, hep-lat/9612011.
3. A. Smilga, *Physics of thermal QCD*, hep-ph/9612347.
4. F.Karsch, Nucl. Phys. Proc. Suppl. **60A** (1998) 169.
5. E. Shuryak and J. Verbaarschot, Nucl. Phys. **A560** (1993) 306.
6. A. Jackson and J. Verbaarschot, Phys. Rev. **D53** (1996) 7223.
7. T. Wettig, A. Schäfer and H. Weidenmüller, Phys. Lett. **B367** (1996) 28.
8. M. Stephanov, Phys. Rev. Lett. **76** (1996) 4472.
9. M. Halasz, A. Jackson and J. Verbaarschot, Phys. Lett. B395 (1997) 293; Phys. Rev. D56 (1997) 5140; M. Halasz, this proceedings.
10. T. Banks and A. Casher, Nucl. Phys. **B169** (1980) 103.
11. J. Osborn, D. Toublan and J. Verbaarschot, hep-th/9806110.
12. M. Berbenni-Bitsch, S. Meyer, A. Schäfer, J. Verbaarschot and T. Wettig, Phys. Rev. Lett. **80** (1998) 1146.
13. J.Z. Ma, T. Guhr and T. Wettig, Eur. Phys. J. **A2** (1998) 87.
14. M. Berbenni-Bitsch, M. Gockeler, T. Guhr, A.D. Jackson, J.Z. Ma, S. Meyer, A. Schäfer, H. Weidenmüller, T. Wettig and T. Wilke, hep-ph/9804439.
15. T. Guhr, J.Z. Ma, S. Meyer and T. Wilke, hep-lat/9806003.
16. M. Berbenni-Bitsch, S. Meyer and T. Wettig, hep-lat/9804030.
17. J. Verbaarschot, Nucl. Phys. **B427** (1994) 434.

18. J. Osborn and J. Verbaarschot, Phys. Rev. Lett. (in press) (1998); Nucl. Phys. **B** (in press) (1998), hep-ph/9803419.
19. M. Halasz and J. Verbaarschot, Phys. Rev. Lett. **74** (1995) 3920.
20. M. Halasz, T. Kalkreuter and J. Verbaarschot, Nucl. Phys. Proc. Suppl. **53** (1997) 266.
21. R. Pullirsch, K. Rabitsch, T. Wettig and H. Markum, hep-ph/9803285.
22. G. Akemann, P. Damgaard, U. Magnea and S. Nishigaki, Nucl. Phys. **B 487**[FS] (1997) 721.
23. E. Brézin, S. Hikami and A. Zee, Nucl. Phys. **B464** (1996) 411.
24. T. Guhr and T. Wettig, Nucl. Phys. **B506** (1997) 589.
25. A. Jackson, M. Sener and J. Verbaarschot, Nucl. Phys. **B479** (1996) 707; Nucl. Phys. **B506** (1997) 612.
26. K. Splittorff and A.D. Jackson, hep-lat/9805018.
27. S. Nishigaki, P. Damgaard and T. Wettig, hep-th/9803007.
28. M. Sener and J. Verbaarschot, Phys. Rev. Lett. (in press), hep-th/9801042.
29. H. Widom, solv-int/9804005.
30. P. Damgaard, Phys. Lett. **B424** (1998) 322; G. Akemann and P. Damgaard, hep-th/9802174; hep-th/9801133.
31. C. Bernard and M. Golterman, Phys. Rev. D49 (1994) 486; C. Bernard and M. Golterman, hep-lat/9311070.
32. T. Guhr, A. Müller-Groeling and H. Weidenmüller, Phys. Rep. **299** (1998) 189.
33. C. Beenakker, Rev. Mod. Phys. **69** (1997) 731.
34. G. Montambaux, cond-mat/9602071.
35. P. Anderson, Phys. Rev. **109** (1958) 1492.
36. T. Schäfer and E. Shuryak, Rev. Mod. Phys. **70** (1998) 323.
37. D. Diakonov and V. Petrov, Nucl. Phys. **B272** (1986) 457.
38. J. Verbaarschot, Phys. Rev. Lett. **72** (1994) 2531; Phys. Lett. **B329** (1994) 351.
39. A. Smilga and J. Verbaarschot, Phys. Rev. **D51** (1995) 829.
40. J. Verbaarschot and I. Zahed, Phys. Rev. Lett. **70** (1993) 3852.
41. D. Fox and P. Kahn, Phys. Rev. **134** (1964) B1152; (1965) 228.
42. T. Nagao and M. Wadati, J. Phys. Soc. Japan **60** (1991) 2998, 3298; **61** (1992) 78, 1910.
43. J. Gasser and H. Leutwyler, Phys. Lett. **188B**(1987) 477.
44. H. Leutwyler and A. Smilga, Phys. Rev. **D46** (1992) 5607.
45. R. Janik, G. Papp, M. Nowak and I. Zahed, hep-ph/9803289.
46. B. Altshuler, I. Zharekeshev, S. Kotochigova and B. Shklovskii, Zh. Eksp. Teor. Fiz. **94** (1988) 343.
47. E. Shuryak, Nucl. Phys. **B302** (1988) 599; D. Diakonov, hep-ph/9602375; J. Stern, hep-ph/9801282.
48. O. Bohigas, M. Giannoni, Lecture notes in Physics **209** (1984) 1; O. Bohigas, M. Giannoni and C. Schmit, Phys. Rev. Lett. **52** (1984) 1.
49. S. Hands and M. Teper, Nucl. Phys. **B347** (1990) 819.
50. T. Kalkreuter, Phys. Lett. **B276** (1992) 485; Phys. Rev. **D48** (1993) 1; Comp. Phys. Comm. **95** (1996) 1.
51. H. Markum, this proceedings.

52. J. Jurkiewicz, M.A. Nowak and I. Zahed, Nucl. Phys. **B478** (1996) 605; G. Papp, Act. Phys. Hung. (1997) 255.
53. H. Hehl and A. Schäfer, hep-ph/9806372.
54. R. Janik, M. Nowak, G. Papp, and I. Zahed, Acta Phys. Polon. B 28 (1997) 2949.
55. I. Barbour, N. Behihil, E. Dagotto, F. Karsch, A. Moreo, M. Stone and H. Wyld, Nucl. Phys. **B275** (1986) 296; M.-P. Lombardo, J. Kogut and D. Sinclair, Phys. Rev. **D54** (1996) 2303.
56. I. Barbour, S. Morrison and J. Kogut, hep-lat/9612012.
57. I. Barbour, S. Morrison, E. Klepfish, J. Kogut and M.-P. Lombardo, hep-lat/9705042.
58. P. Gibbs, Phys. Lett. **B172** (1986) 53.
59. A. Gocksch, Phys. Rev. Lett. **61** (1988) 2054.
60. E. Dagotto, F. Karsch and A. Moreo, Phys. Lett. **169 B**, 421 (1986).
61. P. Gibbs, Phys. Lett. **B182** (1986) 369.
62. J.Ginibre, J.Math.Phys **6** (1965) 440.
63. J. Feinberg and A. Zee, Nucl. Phys. **B504** (1997) 579-608; Nucl. Phys. **B501** (1997) 643.
64. R. Janik, M.A. Nowak, G. Papp and I. Zahed, Nucl. Phys. **B501** (1997) 603.
65. C.N. Yang and T.D. Lee, Phys. Rev. **87** (1952) 104, 410.
66. R. Aloisio, V. Azcoiti, G. Di Carlo, A. Galante, and A. Grillo, hep-lat/9802004; hep-lat/9804020.
67. A.T. Bharucha-Reid and M. Sambandham, *Random Polynomials*, Academic Press, 1986.
68. J. Vink, Nucl. Phys. **B323** (1989) 399.
69. I. Barbour, A. Bell, M. Bernaschi, G. Salina and A. Vladikas, Nucl. Phys. B386 (1992) 683.
70. V. Matteev and R. Shrock, J. Phys. A: Math. Gen. **28** (1995) 5235.
71. D. Bailey, *A Fortran-90 Based Multiprecision System*, NASA Ames RNR Technical Report RNR-94-013.
72. M. Halasz, A. Jackson, R. Shrock, M. Stephanov and J. Verbaarschot, hep-ph/9804290.
73. M. Stephanov, Phys. Lett. **B275** (1996) 249; Nucl. Phys. Proc. Suppl. **53** (1997) 469.
74. G. Akemann, P. Damgaard, U. Magnea and S. Nishigaki, hep-th/9712006.
75. G. Akemann, this proceedings.
76. E. Brézin and S. Hikami, cond-mat/9804023.
77. R. Janik, M. Nowak, G. Papp, and I. Zahed, hep-ph/9804244; G. Papp, this volume.
78. J. Berges and K. Rajagopal, hep-ph/9804233.
79. M. Stephanov, K. Rajagopal and E. Shuryak, hep-ph/9806219.
80. M. Stephanov, this proceedings.
81. Th. Schäfer, Phys. Rev. **D57** (1998) 3950.
82. C. Baillie, K. Bowler, P. Gibbs, I. Barbour and M. Rafique, Phys. Lett. **197B** (1987) 195.
83. M. Halasz, J. Osborn and J. Verbaarschot, Phys. Rev. **D56** (1997) 7059.
84. Y. Fyodorov, B. Khoruzhenko and H. Sommers, Phys. Lett. **A 226** (1997) 46.
85. K. Efetov, Phys. Rev. Lett. **79** (1997) 491; Phys. Rev. **B 56** (1997) 9630.
86. Y. Fyodorov, B. Khoruzhenko and H. Sommers, Phys. Rev. Lett. **79** (1997) 557.